

Carbon-to-Carbon Identity Proton Transfers from Propyne, Acetamide, Thioacetaldehyde, and Nitrosomethane to Their Respective Conjugate Anions in the Gas Phase. An ab Initio Study

Claude F. Bernasconi* and Philip J. Wenzel

Department of Chemistry and Biochemistry of the University of California, Santa Cruz, California 95064

bernasconi@chemistry.ucsc.edu

Received October 31, 2000

Gas-phase acidities of CH_3Y (Y: NO, $\text{C}\equiv\text{CH}$, $\text{CH}=\text{NH}$, and $\text{CH}=\text{S}$), barriers to the identity proton-transfer $\text{CH}_3\text{Y} + \text{CH}_2=\text{Y}^- \rightleftharpoons \text{CH}_2=\text{Y}^- + \text{CH}_3\text{Y}$, as well as geometries and charge distributions of CH_3Y , $\text{CH}_2=\text{Y}^-$ and the transition states of the proton transfers were determined by ab initio methods at the MP2/6-311+G(d,p)/MP2/6-311+G(d,p), B3LYP/6-311+G(d,p), and BPW-91/6-311+G(d,p) levels of theory. The acidities were also calculated at the CCSD(T)/6-311+G(2df,2p) level. To make more meaningful comparisons, the same quantities for previously studied systems (Y: H, $\text{CH}=\text{CH}_2$, $\text{CH}=\text{O}$, CN, NO_2) were recalculated at the levels used in the present work. The geometric parameters as well as the group charges indicate that the transition states for all the reactions are imbalanced, although there is no correlation between the degree of imbalance and the π -acceptor strength of the Y group. Based on multi-parameter correlations with the field (σ_F), resonance (σ_R), and polarizability effect (σ_a) substituent constants, the contributions of each of these effects to the acidities and barriers were evaluated. For the Y groups whose σ_F , σ_R , and σ_a are unknown ($\text{CH}=\text{NH}$, $\text{CH}=\text{S}$, $\text{C}\equiv\text{CH}$), a method for estimating these substituent constants is proposed. The barriers for the $\text{CH}_3\text{Y}/\text{CH}_2=\text{Y}^-$ systems are all lower than for the $\text{CH}_4/\text{CH}_3^-$ system; this contrasts with the situation in solution where the Y groups lead to an increase in the barrier. The reasons for this reversal are analyzed. We also make an attempt to clarify the issue as to why the transition states of these reactions are imbalanced, a question which continues to draw attention in the literature.

Introduction

There is hardly a chemist who does not appreciate the fact that proton transfer is one of the most important elementary reactions in chemistry^{1–3} and biochemistry.⁴ This fact alone would provide enough justification for the intense effort that has been devoted to their study in solution for three-quarters of a century^{1–4} and, more recently, in the gas phase⁵ and by theoretical methods.⁶ But there is an additional reason which makes these processes even more worthwhile as a research target. It is that they involve most of the important features that

characterize polar reactions in general and hence, much of what we learn from the study of proton transfers is applicable to many other polar reactions. For proton transfers from or to carbon, our current focus, these features include the formation and breaking of bonds, the transfer of charge and, in many cases, the delocalization of charge, solvation of products/desolvation of reactants, and the effect of potentially unequal progress in the development of all or some of the above features at the transition state, leading to so-called transition state imbalance or nonsynchronous pathways.^{7–9} Another important feature is that proton transfers often allow the determination of both the rate and equilibrium constants. This is important because it results in the assessment of *intrinsic* rate constants or *intrinsic* barriers,¹⁰ parameters that are at the heart of understanding reactivity.⁹

A type of reaction that is particularly well suited for the computational study of intrinsic barriers and transition state imbalances is the carbon-to-carbon identity proton transfer shown in eq 1 where Y is a π -acceptor group. This is because, due to symmetry, the degree of proton and charge transfer at the transition state is unambiguously defined (50% transfer) and the reaction barrier is the intrinsic barrier. Recent ab initio studies of eq 1^{12–14} (Y: NO_2 , $\text{N}^+\text{O}_2\text{H}$, $\text{CH}=\text{O}$, $\text{CH}=\text{O}^+\text{H}$, CN,

- (1) Eigen, M. *Angew. Chem., Int. Ed. Engl.* **1964**, 3, 1.
- (2) Kresge, A. J. *Acc. Chem. Res.* **1975**, 8, 354.
- (3) (a) Caldin, E. F.; Gold, V., Eds. *Proton-Transfer Reactions*; Wiley & Sons: New York, 1975. (b) Hibbert, F. *Compr. Chem. Kinet.* **1977**, 8, 97.
- (4) (a) Gilbert, H. F. *Biochemistry* **1981**, 20, 5643. (b) Albery, W. J.; Knowles, J. R. *Biochemistry* **1986**, 25, 2572. (c) Kluger, R. *Chem. Rev.* **1990**, 90, 1151. (d) Richard, J. P. In *The Chemistry of Enols*; Rappoport, Z., Ed.; Wiley: New York, 1990; p 651. (e) Gerlt, J. A.; Gassman, P. G. *J. Am. Chem. Soc.* **1993**, 115, 11552.
- (5) (a) Farneth, W. E.; Brauman, J. I. *J. Am. Chem. Soc.* **1976**, 98, 7891. (b) Bowers, M. T., Ed. *Gas-Phase Ion Chemistry*; Academic Press: New York, 1979. (c) Moylan, C. R.; Brauman, J. I. *Annu. Rev. Phys. Chem.* **1983**, 34, 187. (d) Bohme, D. K.; Rakshit, A. B.; Mackay, G. I. *J. Am. Chem. Soc.* **1982**, 104, 1100. (e) Brickhouse, M. D.; Squires, R. R. *J. Am. Chem. Soc.* **1988**, 110, 2706.
- (6) (a) Scheiner, S. *Acc. Chem. Res.* **1985**, 18, 174. (b) McKee, M. L. *J. Am. Chem. Soc.* **1987**, 109, 559. (c) Cybulski, S. M.; Scheiner, S. *J. Am. Chem. Soc.* **1987**, 109, 4199. (d) Scheiner, S. *Acc. Chem. Res.* **1994**, 27, 402. (e) Wolfe, S.; Hoz, S.; Kim, C.-K.; Yang, K. *J. Am. Chem. Soc.* **1990**, 112, 4186. (f) Gronert, S. *J. Am. Chem. Soc.* **1993**, 115, 10258. (g) Bekšic, D.; Bertrán, J.; Lluch, J. M.; Hynes, J. T. *J. Phys. Chem. A* **1998**, 102, 3977. (h) Yamataka, H.; Mustanir; Mishima, M. *J. Am. Chem. Soc.* **1999**, 121, 10223. (i) Van Verth, J. E.; Saunders, W. H., Jr. *Can. J. Chem.* **1999**, 77, 810.

(7) Jencks, D. A. and Jencks, W. P. *J. Am. Chem. Soc.* **1977**, 99, 7948.

(8) Jencks, W. P. *Chem. Rev.* **1985**, 85, 511.

(9) (a) Bernasconi, C. F. *Acc. Chem. Res.* **1987**, 20, 301. (b) Bernasconi, C. F. *Acc. Chem. Res.* **1992**, 25, 9. (c) Bernasconi, C. F. *Adv. Phys. Org. Chem.* **1992**, 27, 119.

(10) The concept of intrinsic barrier was first introduced by Marcus;¹¹ it refers to the barrier of an ergoneutral reaction.



CH=CH₂) have focused on the factors that determine intrinsic barriers and lead to transition state imbalances in the gas phase and how they might differ from those that operate in solution. Two major conclusions from these studies stand out.

(1) The transition states are imbalanced in the sense that charge delocalization from the carbon into the Y group of the *product* ion lags behind, and charge localization from the Y group onto the carbon of the *reactant* anion runs ahead of proton transfer. This means that the lack of synchronization between proton transfer and charge delocalization/localization observed in solution is not just the result of solvation effects. Rather, it is an inherent characteristic of these reactions although solvation probably enhances the transition state imbalances.^{13c}

(2) In contrast to solution reactions, the transition state imbalances do *not* lead to a significant increase in the intrinsic barriers.^{13c}

In this paper we present results of *ab initio* calculations of the CH₃Y/CH₂=Y⁻ systems with Y = NO, CH=NH, CH=S, and C≡CH. We have also recalculated the reactions with Y = NO₂, CH=O, CN, and CH=CH₂ in order to have results at the same computational levels for all systems. Several questions will be addressed. For example: (1) Why is there more charge delocalization in the propyne anion than in the acetonitrile anion despite the greater ability (electronegativity) of nitrogen than carbon to support a negative charge? In the same vein, why is there more delocalization of negative charge in the thioacetaldehyde anion than the acetaldehyde enolate ion? (2) Is polarizability of the Y group an important factor in affecting the acidities of CH₃Y and/or the intrinsic barrier to proton transfer? (3) Is the magnitude of the imbalance correlated with the π -acceptor strength of the Y group? (4) What is the origin of transition state imbalance? This is a question that continues to attract attention. Furthermore, our results will be exploited to estimate the substituent parameters σ_R , σ_F , and σ_a for CH=NH, CH=S, and C≡CH.

Methods and Special Features of Individual Systems

Our calculations have been carried out at the HF/6-311+G(d,p)//HF/6-311+G(d,p) (HF//HF), MP2/6-311+G(d,p)//HF/6-311+G(d,p) (MP2//HF), and MP2/6-311+G(d,p)//MP2/6-311+G(d,p) (MP2//MP2) levels. Gas-phase acidities were recomputed at the CCSD(T)/6-311+G(2df,2p) level. Because of current interest in DFT methods we have also chosen BPW-91/6-311+G(d,p) and B3LYP/6-311+G(d,p). Furthermore, we have recalculated the CH₃NO₂/CH₂=NO₂⁻, CH₃CN/CH₂CN⁻, CH₃CH=O/CH₂=CHO⁻, and CH₃CH=CH₂/CH₂=CHCH₂⁻ reactions at

these levels and using the DFT methods as well. Zero point energy corrections were calculated by scaling the frequencies separate from the scaling of the thermal energy corrections.¹⁵ Partition functions for the thermal corrections were constructed in the Excel spreadsheet program. The values used were as follows: 0.8929 for RHF/6-311+G(d,p) zero point correction, 0.9135 thermal correction, 0.9135 for MP2/6-311+G(d,p) zero point correction, 0.9434 thermal correction, 0.9613 for BPW91 and B3LYP/6-311+G(d,p) zero point correction, 0.9804 for the thermal correction for both of the DFT methods. All calculations were carried out using the GAUSSIAN 94¹⁶ and GAUSSIAN 98¹⁷ suite of programs.

The general method of optimization was the construction and optimization of a Z-matrix input. The carbon acids acetimine, thioacetaldehyde, and nitrosomethane behave as acetaldehyde and nitromethane: the lowest energy conformers (rotamers) all have a single proton eclipsing the electron-withdrawing groups. Reoptimizing in Cartesian coordinates resulted in these eclipsed forms. The results from the Z-matrix optimized structures and those obtained from the G94/G98 default "optimizer" routine were identical.

Staggered and anti-rotamers of our acids required that a hydrogen be fixed at 90.0° (staggered rotamer) or 180.0° (anti-rotamer). Again, Z-matrix input or adding redundant internal coordinates to Cartesian input gave identical structures.

Transition state structures could only be obtained from Z-matrix optimizations with symmetry imposed by assigning variables to the carbon fragments.

Propyne. Neutral propyne is a symmetric top with C_{3v} symmetry. However, symmetry was turned off when optimizing using Cartesian coordinates. The propyne anion was also optimized with Cartesian coordinates as the input. The transition state was optimized using Z-matrix input such that the carbon fragments were arranged in a straight line. The structure was of C_i point group.

Propene. Optimization of propene in its eclipsed, staggered, and anti conformations gave identical results with Z-matrix or Cartesian inputs. The allylic anion proved problematic: at MP2/6-311+G(d,p) the flat conformation gave an imaginary mode (−166 cm^{−1}). Optimization allowing for the terminal carbons to become pyramidal gave a structure such that these carbons gave pyramidal angles of 10.8° without imaginary modes. Only

(15) Scott, A. P.; Radom, L. *J. Phys. Chem. A* **1996**, *41*, 16502.

(16) GAUSSIAN 94, Revision E.2., Frisch, M. J.; Trucks, G. W.; Schlegel, H. B.; Gill, P. M. W.; Johnson, B. G.; Robb, M. A.; Cheeseman, J. R.; Keith, T.; Petersson, G. A.; Montgomery, J. A.; Raghavachari, K.; Al-Laham, M. A.; Zakrzewski, V. G.; Ortiz, J. V.; Foresman, J. B.; Cioslowski, J.; Stevanov, B. B.; Nanayakkara, A.; Challacombe, M.; Peng, C. Y.; Ayala, P. Y.; Chen, W.; Wong, M. W.; Andres, J. L.; Replogle, E. S.; Gomperts, R.; Martin, R. L.; Fox, D. J.; Binkley, J. S.; Defrees, D. J.; Baker, J.; Stewart, J. J. P.; Head-Gordon, M.; Gonzalez, C.; Pople, J. A. Gaussian, Inc., Pittsburgh, PA, 1995.

(17) GAUSSIAN 98, Revision A.7., Frisch, M. J.; Trucks, G. W.; Schlegel, H. B.; Scuseria, G. E.; Robb, M. A.; Cheeseman, J. R.; Zakrzewski, V. G.; Montgomery, J. A., Jr.; Stratmann, R. E., Jr.; Burant, J. C.; Dapprich, S.; Millam, J. M.; Daniels, A. D.; Kudin, K. N.; Strain, M. C.; Farkas, O.; Tomasi, J.; Barone, V.; Cossi, M.; Cammi, R.; Mennucci, B.; Pomelli, C.; Adamo, C.; Clifford, S.; Ochterski, J.; Petersson, G. A.; Ayala, P. Y.; Cui, Q.; Morokuma, K.; Malick, D. K.; Rabuck, A. D.; Raghavachari, K.; Foresman, J. B.; Cioslowski, J.; Ortiz, J. V.; Stefanov, B. B.; Liu, G.; Liashenko, A.; Piskorz, P.; Komaromi, I.; Gomperts, R.; Martin, R. L.; Fox, D. J.; Keith, T.; Al-Laham, M. A.; Peng, C. Y.; Nanayakkara, A.; Gonzalez, C.; Challacombe, M.; Gill, P. M. W.; Johnson, B.; Chen, W.; Wong, M. W.; Andres, J. L.; Gonzalez, C.; Head-Gordon, M.; Replogle, E. S.; Pople, J. A. Gaussian, Inc., Pittsburgh, PA, 1998.

(11) Marcus, R. A. *Annu. Rev. Phys. Chem.* **1964**, *15*, 155. Marcus, R. A. *J. Phys. Chem.* **1968**, *72*, 891.

(12) (a) Saunders, W. H., Jr. *J. Am. Chem. Soc.* **1994**, *116*, 5400. (b) Saunders, W. H., Jr.; Van Verth, J. E. *J. Org. Chem.* **1994**, *60*, 3452.

(13) (a) Bernasconi, C. F.; Wenzel, P. J. *J. Am. Chem. Soc.* **1994**, *116*, 5405. (b) Bernasconi, C. F.; Wenzel, P. J. *J. Am. Chem. Soc.* **1996**, *118*, 10494. (c) Bernasconi, C. F.; Wenzel, P. J.; Keeffe, J. R.; Gronert, S. *J. Am. Chem. Soc.* **1997**, *119*, 4008.

(14) Lee, I.; Kim, C. K.; Kim, C. K. *J. Phys. Org. Chem.* **1999**, *12*, 255.

Table 1. Gas-Phase Acidities, ΔH° , and Barriers ΔH^\ddagger ^{a,b}

| acid | RHF ^c | MP2 ^d | B3LYP | BPW91 | CCSD(T)/ 6-311+G(2df,2p) | $\Delta H^\circ_{\text{exp}}$ ^e |
|------------------------------------|------------------|------------------|-------------|---------------|-----------------------------|--|
| ΔH° | | | | | | |
| CH ₄ | 424.1 | 418.1 | 415.8 | 415.5 | 418.0 | 416.6 ± 0.8 |
| CH ₃ CH=CH ₂ | 398.7 | 390.2 | 387.0 | 383.7 | 391.2 | 390.7 ± 2.4 |
| CH ₃ C≡CH | 390.9 | 385.9 | 379.2 | 377.6 | 384.0 | 382.4 ± 2.6 |
| CH ₃ C≡N | 379.9 | 375.4 | 370.3 | 369.9 | 374.8 | 372.9 ± 2.6 |
| CH ₃ CH=NH(anti) | 388.7 | 379.8 | 377.0 | 376.2 | 380.1 | |
| CH ₃ CH=NH(syn) | 385.2 | 376.1 | 374.2 | 373.5 | 377.0 | |
| CH ₃ CH=O | 374.9 | 367.2 | 363.5 | 362.9 | 367.3 | 365.8 ± 2.9 |
| CH ₃ NO ₂ | 363.0 | 359.0 | 352.4 | 354.0 | 359.1 | 356.4 ± 2.9 |
| CH ₃ NO | 361.7 | 351.9 | 346.7 | 346.0 | 352.9 | |
| CH ₃ CH=S | 346.2 | 348.7 | 343.4 | 344.4 | 347.2 | |
| ΔH^\ddagger | | | | | | |
| CH ₄ | 19.4 (20.3) | 8.1 (12.1) | 6.7 (7.9) | 3.5 (4.9) | | |
| CH ₃ CH=CH ₂ | 21.3 (22.0) | 4.7 (8.2) | 5.2 (5.8) | 2.3 (3.0) | | |
| CH ₃ C≡CH | 17.4 (18.1) | 1.8 (5.3) | 4.3 (4.9) | 0.6 (1.2) | | |
| CH ₃ C≡N | 3.8 (4.6) | -8.5 (-5.2) | -8.3 (-7.8) | -12.2 (-11.6) | | |
| CH ₃ CH=NH(anti) | 19.3 (20.0) | 2.9 (6.2) | 2.4 (3.0) | -3.1 (-2.4) | | |
| CH ₃ CH=NH(syn) | 16.1 (16.8) | 0.3 (2.8) | 0.0 (0.6) | -5.8 (-5.2) | | |
| CH ₃ CH=O | 15.4 (16.0) | -0.3 (2.7) | -1.8 (-1.3) | 0.5 (1.1) | | |
| CH ₃ NO ₂ | 9.3 (10.7) | -6.2 (-2.8) | -7.8 (-7.2) | -13.0 (-12.4) | | |
| CH ₃ NO | 18.8 (19.5) | -1.1 (2.1) | -4.4 (-3.9) | -11.5 (-10.8) | | |
| CH ₃ CH=S | 19.3 (20.1) | 0.3 (4.1) | -0.8 (-0.3) | 3.0 (3.5) | | |

^a In kcal/mol. ^b ΔH^\ddagger refers to difference between the transition state and separated reactants. ^c HF//HF. ^d MP2//MP2. ^e Reference 32. ^f Numbers in parentheses refer to ΔH^\ddagger corrected for BSSE.

at MP2 was this pyramidalization detected; at all other levels the allyl anion is flat. The transition state for identity proton transfer gave a secondary imaginary mode (-5 cm^{-1}) but only at the MP2 level. This was treated as a free degree of freedom (no contribution to the zero point energy, RT to the thermal correction).

Acetonitrile. The neutral species is of C_{3v} symmetry point group. Each of the hydrogens are identical and optimization in internal coordinates is identical with that achieved by the GAUSSIAN 94 internal optimizer routine. The anion of acetonitrile is nonplanar with a significant pyramidal angle of 36.5° . A transition structure is found when this anion is forced into a planar configuration. It appears then that inversion of this pyramidal anion proceeds with a very small barrier of $<0.5\text{ kcal}$ through the computed planar structures.

The transition state for the acetonitrile identity proton-transfer optimized in Z-matrix coordinates resulted in the carbon fragments forming a linear structure.

Acetimine. Syn and anti N–H isomeric systems were independently explored, and treated as separate systems of reactants, transition state, and products. No attempt was made to determine the rotational barrier for the N–H group although the anti conformer is the more stable reactant and the syn the more stable anion.

The transition states and anions for these conformers were optimized in Z-matrix form. The anion for the N–H anti conformer at MP2//MP2 yielded a planar structure with a single negative frequency associated with pyramidalization of the methylene carbon. Since this was not observed at any other level and the negative frequency was small (-50.1 cm^{-1}), this was treated as a free degree of motion, with no contribution to the zero-point energy at 0 K but an RT contribution to the vibrational heat capacity.

Thioacetaldehyde. Z-matrix inputs were used initially. For reactants and products the Z-matrix optimization was indistinguishable from the GAUSSIAN 94 optimizer result. The transition state was optimized in Z-matrix coordinates only, with an enforced C_i symmetry point group and the center of inversion placed through

the transferred proton. All reactant and product geometries were determined to be stable species, i.e., only real vibrational modes were found.

Nitrosomethane. As in the thioacetaldehyde case, nitrosomethane and its anion were optimized with Z-matrix inputs and reoptimized from Cartesian coordinates without change. Two transition state structures were examined. With respect to each other the N=O groups can be arranged with syn or anti. The anti configuration was observed to be of lower energy and is the one discussed in this paper.

The tautomeric species $\text{CH}_2=\text{C}=\text{NH}$, $\text{CH}_2=\text{C}=\text{CH}_2$, $\text{CH}_2=\text{CHOH}$, $\text{CH}_2=\text{CHSH}$, $\text{CH}_2=\text{CHNH}_2$, $\text{CH}_2=\text{NO}_2\text{H}$, and $\text{CH}_2=\text{NOH}$ were calculated from the corresponding anion with a hydrogen ion added. Optimization was performed using the internal optimizer in the GAUSSIAN program.

The multiparameter fits (Figures 1 and 3) were generated by construction of matrixes for the σ_F , σ_R , and σ_α parameters and manipulating that matrix with a matrix of either the gas-phase acidities or the barriers.¹⁸ The use of "Solver" in the Excel spreadsheet gave excellent agreement with our matrix method.

Results and Discussion

General Features. Table 1 summarizes the gas-phase acidities (ΔH°) at various computational levels. Absolute energies and zero point energies of the various species involved are reported in Table S1 of the Supporting Information.¹⁹ The quality of the calculations may be judged by a comparison with experimental gas-phase acidities or, for the cases where no experimental values are available, with those calculated at the CCSD(T)/6-311+G(2df,2p) level. By these criteria, the quality of the MP2//MP2 and B3LYP calculations are better than the BPW91 calculations, with MP2//MP2 slightly underesti-

(18) Mendenhall, W.; Schaeffer, R. L.; Wackerly, D. D. *Mathematical Statistics with Applications*; Duxbury Press: Boston, MA, 1981; p 430.

(19) See paragraph concerning Supporting Information at the end of this paper.

Table 2. Bond Lengths and Pyramidal Angles^a (MP2/6-311+G(d,p))

| | neutral | anion | TS | % progress at TS |
|---|---------|--------|--------|------------------|
| CH₃C≡N | | | | |
| <i>r</i> _{C-C} | 1.463 | 1.403 | 1.431 | |
| Δr_{C-C} | | -0.060 | -0.032 | 53.3 |
| <i>r</i> _{C=N} | 1.174 | 1.195 | 1.185 | |
| $\Delta r_{C=N}$ | | 0.021 | 0.011 | 52.4 |
| α | 54.12 | 36.91 | 50.48 | |
| $\Delta\alpha$ | | -17.21 | -3.64 | 21.2 |
| CH₃C=CH | | | | |
| <i>r</i> _{C-C} | 1.464 | 1.366 | 1.430 | |
| Δr_{C-C} | | -0.098 | -0.034 | 34.7 |
| <i>r</i> _{C=C} | 1.218 | 1.281 | 1.236 | |
| $\Delta r_{C=C}$ | | 0.063 | 0.018 | 28.6 |
| α | 53.09 | 0.00 | 47.82 | |
| $\Delta\alpha$ | | -53.09 | -5.27 | 9.92 |
| CH₃CH=CH₂ | | | | |
| <i>r</i> _{C-C} | 1.502 | 1.399 | 1.444 | |
| Δr_{C-C} | | -0.103 | -0.058 | 56.3 |
| <i>r</i> _{C=C} | 1.341 | 1.399 | 1.368 | |
| $\Delta r_{C=C}$ | | 0.058 | 0.027 | 46.6 |
| α | 53.22 | 0.00 | 41.19 | |
| $\Delta\alpha$ | | -53.22 | -12.03 | 22.6 |
| CH₃CH=NH (syn) | | | | |
| <i>r</i> _{C-C} | 1.505 | 1.398 | 1.440 | |
| Δr_{C-C} | | -0.107 | -0.061 | 57.0 |
| <i>r</i> _{C=N} | 1.282 | 1.340 | 1.311 | |
| $\Delta r_{C=N}$ | | 0.058 | 0.029 | 50.0 |
| α | 54.60 | 0.00 | 40.49 | |
| $\Delta\alpha$ | | -54.60 | -14.11 | 25.8 |
| CH₃CH=NH (anti) | | | | |
| <i>r</i> _{C-C} | 1.498 | 1.391 | 1.432 | |
| Δr_{C-C} | | -0.107 | -0.066 | 61.7 |
| <i>r</i> _{C=N} | 1.280 | 1.344 | 1.315 | |
| $\Delta r_{C=N}$ | | 0.064 | 0.035 | 54.7 |
| α | 54.37 | 0.00 | 39.39 | |
| $\Delta\alpha$ | | -54.37 | -14.98 | 27.6 |
| CH₃CH=O^b | | | | |
| <i>r</i> _{C-C} | 1.503 | 1.391 | 1.430 | |
| Δr_{C-C} | | -0.112 | -0.073 | 65.2 |
| <i>r</i> _{C=O} | 1.215 | 1.271 | 1.246 | |
| $\Delta r_{C=O}$ | | 0.056 | 0.031 | 55.4 |
| α | 51.55 | 0.00 | 37.32 | |
| $\Delta\alpha$ | | -51.55 | 14.23 | 27.6 |
| CH₃CH=S | | | | |
| <i>r</i> _{C-C} | 1.499 | 1.365 | 1.413 | |
| Δr_{C-C} | | -0.134 | -0.086 | 64.2 |
| <i>r</i> _{C=S} | 1.618 | 1.726 | 1.668 | |
| $\Delta r_{C=S}$ | | 0.108 | 0.050 | 46.3 |
| α | 55.54 | 0.00 | 42.34 | |
| $\Delta\alpha$ | | -55.54 | -13.20 | 23.8 |
| CH₃NO₂^c | | | | |
| <i>r</i> _{C-N} | 1.493 | 1.356 | 1.414 | |
| Δr_{C-N} | | -0.137 | -0.079 | 57.7 |
| <i>r</i> _{N=O} | 1.230 | 1.278 | 1.253 | |
| $\Delta r_{N=O}$ | | 0.048 | 0.023 | 47.9 |
| α | 59.00 | 13.40 | 46.80 | |
| $\Delta\alpha$ | | -45.6 | -12.2 | 26.8 |
| CH₃NO | | | | |
| <i>r</i> _{C-N} | 1.480 | 1.320 | 1.368 | |
| Δr_{C-N} | | -0.160 | -0.112 | 70.0 |
| <i>r</i> _{N=O} | 1.220 | 1.301 | 1.257 | |
| $\Delta r_{N=O}$ | | 0.081 | 0.037 | 45.7 |
| α | 60.57 | 0.00 | 33.94 | |
| $\Delta\alpha$ | | -60.57 | -26.63 | 44.0 |

^a Pyramidal angle of CH₃(CH₂) carbon. ^b Reference 13b. ^c Reference 13c.

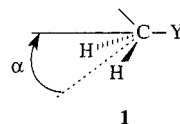
matings and B3LYP slightly overestimating the acidities. In our following discussions we will mainly focus on the results obtained at the MP2//MP2 level which, overall, appears to give the most reliable results.

Table 3. NPA Group Charges (MP2//MP2)

| group | neutral | anion | difference ^a | TS | difference ^b |
|--|---------|--------|-------------------------|--------|-------------------------|
| CH₃C≡N | | | | | |
| CH ₃ (CH ₂) | 0.041 | -0.644 | -0.685 | -0.446 | -0.487 |
| C≡N | -0.041 | -0.356 | -0.315 | -0.206 | -0.165 |
| H (transferred) | | | | 0.303 | |
| CH₃C=CH | | | | | |
| CH ₃ (CH ₂) | 0.028 | -0.463 | -0.491 | -0.429 | -0.457 |
| C=CH | -0.028 | -0.537 | -0.509 | -0.219 | -0.191 |
| H (transferred) | | | | 0.296 | |
| CH₃CH=CH₂ | | | | | |
| CH ₃ (CH ₂) | 0.003 | -0.461 | -0.464 | -0.376 | -0.379 |
| CH=CH ₂ | -0.003 | -0.539 | -0.536 | -0.266 | -0.263 |
| H (transferred) | | | | 0.285 | |
| CH₃CH=NH (syn) | | | | | |
| CH ₃ (CH ₂) | -0.013 | -0.493 | -0.480 | -0.398 | -0.385 |
| CH=NH | 0.013 | -0.507 | -0.520 | -0.248 | -0.261 |
| H (transferred) | | | | 0.293 | |
| CH₃CH=NH (anti) | | | | | |
| CH ₃ (CH ₂) | 0.004 | -0.452 | -0.456 | -0.366 | -0.370 |
| CH=NH | -0.004 | -0.548 | -0.544 | -0.281 | -0.277 |
| H (transferred) | | | | 0.293 | |
| CH₃CH=O | | | | | |
| CH ₃ (CH ₂) | -0.021 | -0.469 | -0.448 | -0.384 | -0.363 |
| CH=O | 0.021 | -0.531 | -0.522 | -0.266 | -0.287 |
| H (transferred) | | | | 0.301 | |
| CH₃CH=S | | | | | |
| CH ₃ (CH ₂) | 0.021 | -0.244 | -0.265 | -0.233 | -0.254 |
| CH=S | -0.021 | -0.756 | -0.735 | -0.413 | -0.392 |
| H (transferred) | | | | 0.291 | |
| CH₃NO₂ | | | | | |
| CH ₃ (CH ₂) | 0.244 | -0.146 | -0.390 | -0.093 | -0.337 |
| NO ₂ | -0.244 | -0.854 | -0.610 | -0.535 | -0.291 |
| H (transferred) | | | | 0.253 | |
| CH₃NO | | | | | |
| CH ₃ (CH ₂) | 0.155 | -0.134 | -0.289 | -0.082 | -0.237 |
| NO | -0.155 | -0.866 | -0.711 | -0.548 | -0.393 |
| H (transferred) | | | | 0.260 | |

^a Difference between anion and neutral. On Y-group this difference corresponds to $-\chi$ in eqs 12–14. ^b Difference between TS and neutral; it corresponds to $-\delta_C$ and $-\delta_Y$ in eqs 12–14, respectively.

Table 2 provides a summary of the bond lengths and angles that are most relevant to the questions addressed in this study. For more complete data on geometric parameters see Figure S1.¹⁹ The pyramidal angle α is defined as shown in **1** where the solid line is the projection of the C–Y bond and the dashed line is the



bisector of the HCH groups. Note that for a planar molecule or ion α is zero.

Table 3 reports group charges calculated by the NPA method²⁰ at the MP2//MP2 level. Most group charges calculated by the Mulliken method, as well as the NPA or Mulliken charges obtained from B3LYP calculations, are quite similar to the NPA-MP2//MP2 group charges. They are summarized in Table S2,¹⁹ along with charges on the individual atoms.

Resonance Effects on Acidities. As has been shown for several examples, in particular CH₃CH=O,^{12a,12b,21}

(20) Reed, A. E.; Curtiss, L. A.; Weinhold, F. *Chem. Rev.* **1988**, *88*, 899.

(21) Wiberg, K. B.; Castejon, H. *J. Org. Chem.* **1995**, *60*, 6327.

Table 4. Anions: Relative C–Y Bond Contraction^a and Negative Charge on Y-Group^b

| | σ_R^c | $100 \times \Delta r_{C-Y}^d / r_{C-Y}$ | charge on Y | χ^e |
|------------------------------------|--------------------|---|-------------|----------|
| CH ₃ C≡N | 0.10 | 4.10 | −0.356 | 0.355 |
| CH ₃ C≡CH | ≈0.15 ^d | 6.69 | −0.537 | 0.509 |
| CH ₃ CH=CH ₂ | 0.16 | 6.86 | −0.539 | 0.535 |
| CH ₃ CH=NH (syn) | ≈0.17 ^d | 7.11 | −0.507 | 0.520 |
| CH ₃ CH=NH (anti) | ≈0.17 ^d | 7.14 | −0.548 | 0.543 |
| CH ₃ CH=O | 0.19 | 7.64 | −0.531 | 0.552 |
| CH ₃ CH=S | ≈0.33 ^d | 8.94 | −0.756 | 0.735 |
| CH ₃ NO ₂ | 0.18 | 9.18 | −0.854 | 0.610 |
| CH ₃ NO | 0.26 | 10.8 | −0.866 | 0.711 |

^a MP2/6-311+G(d,p). ^b NPA at MP2//MP2. ^c Taft's²³ gas-phase resonance substituent constants. ^d Estimated, see text. ^e Difference between charge on Y in the anion and that on Y in CH₃Y (eqs 12–14).

CH₃NO₂,^{13c,22} and CH₃CH=CH₂,^{12b} resonance stabilization of the carbanion by delocalization of the negative charge into the Y-group plays a dominant role in determining the acidities of most carbon acids activated by π -acceptors. The present study now shows this to be the case as well for CH₃C≡CH, CH₃CH=NH, CH₃NO, and CH₃CH=S which have not been investigated before.

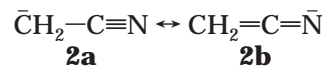
Our calculations provide two independent methods for assessing the degree of charge delocalization. One is the amount of charge on the Y group relative to that on the CH₂ group of the anion; the other is the degree of C–Y bond contraction upon converting CH₃Y into its anion. These measures are summarized in Table 4 for the MP2//MP2 calculations. The results of the B3LYP calculations which are very similar to those for the MP2 calculations are reported in Table S3.¹⁹

The rank order of increasing charge delocalization into the Y-group based on bond contractions is CN \ll C≡CH \sim CH=CH₂ < CH=NH(syn) \sim CH=NH(anti) < CH=O \ll CH=S < NO₂ \ll NO. For those Y groups for which gas phase σ_R substituent constants²³ are available this order is also reflected in the σ_R values except for a change in rank between NO₂ and CH=O, i.e., CN (0.10) \ll CH=CH₂ (0.16) < NO₂ (0.18) < CH=O (0.19) \ll NO (0.26).

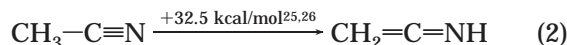
The rank order based on the charges is CN \ll CH=NH(syn) < CH=O < C≡CH \sim CH=CH₂ \sim CH=NH(anti) \ll CH=S < NO₂ < NO. This is quite similar to the rank order based on bond contractions, i.e., the CN is at the low end, CH=S, NO₂, and NO are at the high end, while the other five groups are all close with just slight differences in rank order compared to that based on bond contractions.

There are a number of noteworthy features regarding the relative π -acceptor strength of some of the Y groups which need to be addressed. (1) One is a comparison between CH₃CN and CH₃C≡CH. As has been noted before,^{12b,21} there is much less charge delocalization in CH₂CN[−] than in all the other anions (Table 3). This is even reflected in the nonplanar geometry of CH₂CN[−] (α = 36.9°) According to Richard et al.,²⁴ a major impediment to the delocalization of the anionic charge into the cyano group is the inherent instability of the cumulative double bonds in **2b**. This leads to a preference

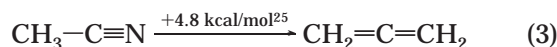
of resonance structure **2a** despite the greater electronegativity of nitrogen. In support of this interpretation,



Richard et al.²⁴ cite the much higher energy of ketenimine relative to acetonitrile (eq 2).

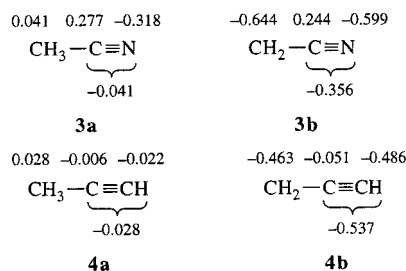


The situation for the propyne anion is quite different. The C–Y bond contraction is substantially larger than for CH₂CN[−], and the anionic charge is more evenly distributed between the CH₂ and C≡CH groups. In view of the smaller electronegativity of carbon compared to nitrogen one might have expected the opposite behavior, i.e., even less delocalization into the C≡CH group. However, the much smaller energy difference between propyne and allene (eq 3) than between acetonitrile and



ketenimine indicates that the cumulative double bonds in allene are not nearly as detrimental as in ketenimine. This may, in large measure, reflect the fact that the stability of a C≡N triple bond (\approx 213 kcal/mol)²⁷ relative to a C=N double bond (\approx 147 kcal/mol)²⁷ is higher than the stability of a C≡C triple bond (\approx 200 kcal/mol)²⁷ relative to a C=C double bond (\approx 146 kcal/mol).²⁷

With respect to charges, the group charge on the CN group (−0.356) of CH₂CN[−] is smaller than that on the C≡CH group (−0.537) of CH₂CCH[−], consistent with the respective bond contractions. On the other hand, the breakdown of the group charges into their components (**3b** and **4b**) shows more charge on N in CH₂CN[−] than on CH in CH₂CCH[−]. Unless this is an artifact of



how charges are apportioned in our calculations,²⁸ this result may be viewed as being consistent with the stronger field effect of the more electronegative nitrogen.

An additional point of interest is a comparison of the change in the charge on the nitrogen when converting acetonitrile (**3a**) into its anion (−0.281) with that on the terminal CH group for the conversion of propyne into its anion (−0.464). The relatively small change for acetonitrile is another indication that the loss of the C≡N triple bond character is much smaller than that of the C≡CH triple bond.

(22) Lammertsma, K.; Prasad, B. V. *J. Am. Chem. Soc.* **1993**, *115*, 2348.

(23) (a) Taft, R. W.; Topsom, R. D. *Prog. Phys. Org. Chem.* **1987**, *16*, 1. (b) Hansch, C.; Leo, A.; Taft, R. W. *Chem. Rev.* **1991**, *91*, 165.

(24) Richard, J. P.; Williams, G.; Gao, J. *J. Am. Chem. Soc.* **1999**, *121*, 715.

(25) At MP2//MP2, this work.

(26) Richard et al.²⁴ report a Gibbs free energy of 28.3 kcal/mol.

(27) Streitwieser, A.; Heathcock, C. H.; Kosower, E. M. *Introduction to Organic Chemistry*, 4th ed.; Macmillan: New York, 1992; p A5.

(28) Hehre, W. J.; Radom, L.; Schleyer, P. v. R.; Pople, J. A. *Ab Initio Molecular Orbital Theory*; Wiley-Interscience: New York, 1986; p 336.

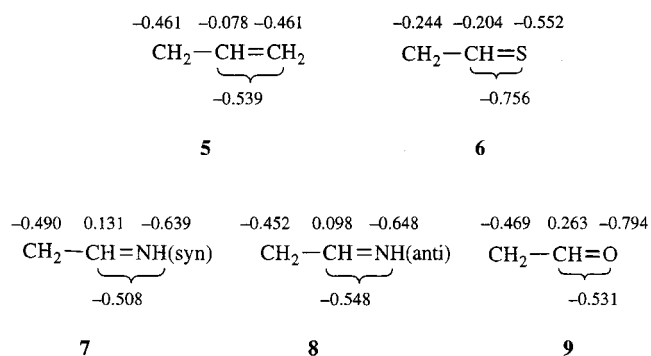
Table 5. Dissection of the Contributions of Field, Resonance and Polarizability Effects to ΔH° ^a and ΔH^\ddagger ^{a,b}

| CH ₃ Y | σ_F | σ_R | σ_α | $\Delta\Delta H^\ddagger$ (eq 11) | | | ΔH^\ddagger ^c | $\Delta\Delta H^\ddagger$ (eq 15) | | | ΔH^\ddagger ^c |
|---|------------|------------|-----------------|-----------------------------------|------------------------|----------------------------------|----------------------------------|-----------------------------------|---------------------------|-------------------------------------|----------------------------------|
| | | | | $\rho_F^\circ\sigma_F$ | $\rho_R^\circ\sigma_R$ | $\rho_\alpha^\circ\sigma_\alpha$ | | $\rho_F^\ddagger\sigma_F$ | $\rho_R^\ddagger\sigma_R$ | $\rho_\alpha^\ddagger\sigma_\alpha$ | |
| Y Groups with Known σ_F , σ_R , and σ_α Values | | | | | | | | | | | |
| CH ₄ | 0 | 0 | 0 | 0 | 0 | 0 | 418.1 (418.6) | 0 | 0 | 0 | 8.05 (8.08) |
| CH ₃ CH=CH ₂ | 0.06 | 0.16 | −0.50 | −2.6 | −30.8 | 2.3 | 390.2 (387.5) | −1.4 | 1.6 | −3.8 | 4.65 (4.50) |
| CH ₃ CN | 0.60 | 0.10 | −0.46 | −25.8 | −19.2 | 2.1 | 375.4 (375.7) | −13.6 | 1.0 | −3.5 | −8.46 (−7.98) |
| CH ₃ CH=O | 0.31 | 0.19 | −0.46 | −13.3 | −36.6 | 2.1 | 367.2 (370.8) | −7.0 | 1.9 | −3.5 | −0.31 (−0.55) |
| CH ₃ NO ₂ | 0.65 | 0.18 | −0.26 | −27.9 | −34.6 | 1.2 | 359.0 (357.2) | −14.7 | 1.8 | −2.0 | −6.16 (−6.81) |
| CH ₃ NO | 0.41 | 0.26 | −0.25 | −17.6 | −50.0 | 1.2 | 351.9 (352.1) | −9.3 | 2.6 | −1.9 | −1.06 (−0.53) |
| Y Groups with Estimated σ_F , σ_R , and σ_α values ^d | | | | | | | | | | | |
| CH ₃ C≡CH | 0.14 | 0.15 | −0.40 | −6.0 | −28.9 | 1.8 | 385.9 (385.5) | −3.2 | 1.5 | −3.0 | 1.75 (3.38) |
| CH ₃ CH=NH(syn) | 0.27 | 0.17 | −0.45 | −11.6 | −32.7 | 2.1 | 376.1 (376.4) | −6.1 | 1.7 | −3.4 | 0.30 (0.28) |
| CH ₃ CH=NH(anti) | 0.20 | 0.17 | −0.40 | −8.6 | −32.7 | 1.8 | 379.8 (379.1) | −4.5 | 1.7 | −3.0 | 2.90 (2.28) |
| CH ₃ CH=S | 0.22 | 0.33 | −0.75 | −9.5 | −63.5 | 3.4 | 348.7 (349.0) | −5.0 | 3.2 | −5.7 | 0.32 (0.58) |

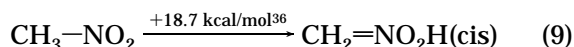
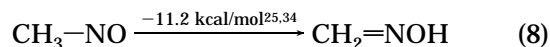
^a In kcal/mol at MP2//MP2 level. ^b ΔH^\ddagger refers to difference in enthalpy between the transition state and separated reactants. ^c Number in parentheses: from correlation according to eq 11 (ΔH°) with $\Delta\Delta H^\circ = -43.0\sigma_F - 192.5\sigma_R - 4.60\sigma_\alpha$ or eq 15 (ΔH^\ddagger) with $\Delta\Delta H^\ddagger = -22.6\sigma_F - 9.81\sigma_R + 7.59\sigma_\alpha$, respectively. ^d σ_F , σ_R , and σ_α estimated as described in text.

(2) The Y groups CH=CH₂, CH=NH, CH=O, and CH=S represent another set of similar structures. By the criterion of C–Y bond contraction, their π -acceptor strength increases in the order CH=CH₂ \leq CH=NH(syn) \sim CH=NH(anti) $<$ CH=O \ll CH=S. Just as in the comparison between C≡CH and C≡CN, the π -acceptor strength does not follow electronegativity; this is particularly striking for CH=O vs CH=S since S has the lowest and O the highest electronegativity.²⁹ Again, relative tautomerization energies, eqs 4–7, are revealing. They show that conversion of a C=X double bond to a

groups (5–9) essentially reflect the electronegativities,³³ except for X = S.



(3) A third revealing comparison is that between CH₃NO₂ and CH₃NO. The relative C–N bond contractions in the anions are NO > NO₂ and the NO group carries a slightly larger negative charge than the NO₂ group. Once again, there seems to be a connection with relative tautomerization energies, i.e., CH₂=NOH is more stable relative to CH₃NO while CH₂=NO₂H is less stable relative to CH₃NO₂, eqs 8 and 9.



Field and Polarizability Effects on Acidities. In a previous study we showed that the field effect is the second most important factor affecting the acidities of CH₃CH=O and CH₃NO₂, the most important factor for CH₃CN, and of little importance for CH₃CH=CH₂.^{13c} This conclusion was based on a correlation of $\Delta\Delta H^\circ = \Delta H^\circ(\text{CH}_3\text{Y}) - \Delta H^\circ(\text{CH}_4)$ with σ_F and σ_R according to eq 10 where σ_F is the gas-phase field effect substituent parameter²³ of the Y group.

$$\Delta\Delta H^\circ = \rho_F^\circ\sigma_F + \rho_R^\circ\sigma_R \quad (10)$$

The least squares correlation for CH₄, CH₃CH=CH₂, CH₃CN, CH₃CH=O, and CH₃NO₂ yielded $\rho_R^\circ = -177.8$ and $\rho_F^\circ = -45.5$.³⁷ Although the correlation based just on

(33) As in the comparison between CH₂CN[−] and CH₂CCH[−], the possibility that the charges on the terminal groups are an artifact of how the charges are apportioned²⁸ cannot be excluded.

C–X single bond is less favorable when X is more electronegative than carbon, at least for X = NH and X = O, reflecting the greater increase in C=X double bond strength relative to the C–X single bond strength with increasing electronegativity of X.³¹ In the case of CH₃CH=S, the larger size of the sulfur atom probably contributes to the stabilization of the negative charge in the anion; this is similar to the greater stabilization of CH₃S[−] compared to CH₃O[−], as reflected in the much stronger gas-phase acidity of CH₃SH (350.6 kcal/mol) compared to CH₃OH (380.6 kcal/mol).³²

With respect to the charges, the situation is again similar to that for the comparison between CH₂CN[−] and CH₂CCH[−], i.e., the *group* charges follow a similar pattern as the bond contractions, but the charges on the terminal

(29) The electronegativities are S (2.4), C (2.5), N (3.1), O (3.5).³⁰

(30) Streitwieser, A.; Heathcock, C. H.; Kosower, E. M. *Introduction to Organic Chemistry*, 4th ed.; MacMillan: New York, 1992; p 161.

(31) For example, the difference in bond dissociation energies (in kcal/mol) for C=O (176) vs C–O (86) is much larger than for C=C (146) vs C–C (83).²⁷

(32) Lias, S. G.; Bartmess, J. E.; Liebman, J. E.; Levin, R. D.; Holmes, J. L.; Mallard, W. G. *J. Phys. Chem. Ref. Data* **1998**, *17*, Suppl. 1.

field and resonance effects was remarkably good ($r^2 = 0.986$), it neglected polarizability effects. Because such effects can potentially be quite important, especially for gas-phase anions^{38,39} but also in solution,⁴⁰ we have now added the polarizability term $\rho_\alpha^\circ\sigma_\alpha$ to our correlation (eq 11). This is shown in Figure 1. The correlation which

$$\Delta\Delta H^\circ = \rho_F^\circ\sigma_F + \rho_R^\circ\sigma_R + \rho_\alpha^\circ\sigma_\alpha \quad (11)$$

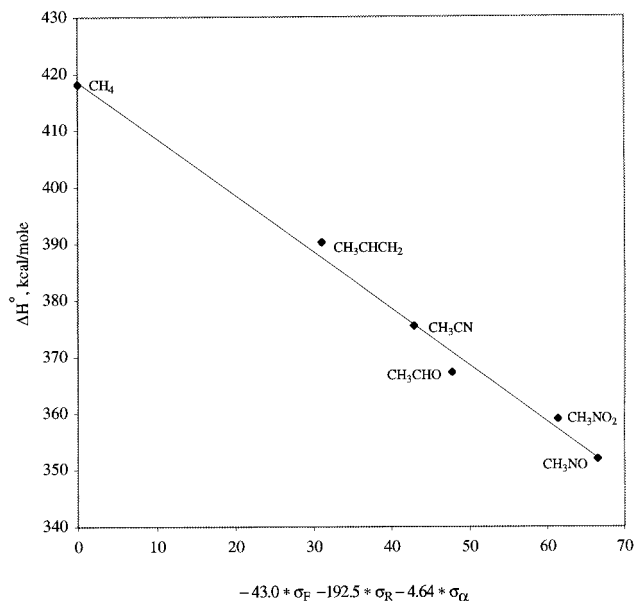


Figure 1. Plot of ΔH° vs $\rho_F^\circ\sigma_F + \rho_R^\circ\sigma_R + \rho_\alpha^\circ\sigma_\alpha$; ρ -values obtained by least-squares fitting ($r^2 = 0.992$, intercept = 418.6).

now also includes CH₃NO is excellent ($r^2 = 0.992$) and yields $\rho_F^\circ = -43.0$, $\rho_R^\circ = -192.5$, and $\rho_\alpha^\circ = -4.64$; for the B3LYP acidities one obtains $\rho_F^\circ = -48.0$, $\rho_R^\circ = -197$, and $\rho_\alpha^\circ = -5.96$ ($r^2 = 0.995$, Figure S2¹⁹). The ρ_R° and ρ_F° values are not significantly different from the previous ones which is not surprising since ρ_α° is very small, indicating that polarizability is of minor importance. This small role played by polarizability in the present systems implies that its effect is greatly diminished when the anionic charge mainly resides on the Y-group rather than the CH₂-group, as is the case for all our anions except for CH₂CN⁻. In fact, because the σ_α values are defined as negative numbers,²³ the slightly negative ρ_α° suggests a small anion destabilizing effect; however, in view of the smallness of the effect, not much significance should be attached to this result.

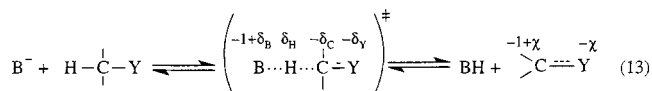
A clearer indication of the absolute and relative contributions of field, resonance and polarizability effects to the acidity of the various compounds can be obtained by calculating the individual $\rho_F^\circ\sigma_F$, $\rho_R^\circ\sigma_R$ and $\rho_\alpha^\circ\sigma_\alpha$ terms for each acid rather than just looking at the ρ_F° , ρ_R° and ρ_α° values, respectively. These terms are summarized in Table 5 for all systems of this study; for the compounds with Y groups with unknown substituent constants (C≡

CH, CH=NH, and CH=S), these terms were estimated based on approximate substituent constants estimated as described in a later section. The information in Table 5 is quite revealing. For example, the resonance contribution amounts to about -63 kcal/mol for CH₃CH=S, -50 kcal/mol for CH₃NO, is in the range of -29 to -36 kcal/mol for CH₃CH=CH₂, CH₃C≡CH, CH₃CH=NH, CH₃CH=O, and CH₃NO₂, and a mere -19 kcal/mol for CH₃CN. On the other hand, the field effect contribution for CH₃CN (-26 kcal/mol) is larger than for any of the other compounds except for CH₃NO₂ (-27 kcal/mol), and for CH₃C≡CH (-6 kcal/mol) and CH₃CH=CH₂ (-2.6 kcal/mol) it is very small to almost negligible. The polarizability effect, if there is any significance to it all, is seen to lower the acidities by a mere 2.1 to 3.4 kcal/mol for CH₃CH=CH₂, CH₃CN, CH₃CH=O, and CH₃CH=S, and even less (1.2 kcal/mol) for CH₃NO₂ and CH₃NO.

Transition State Structure. Relevant geometric parameters and group charges are summarized in Tables 2 and 3, respectively. There are three quantities that are of particular relevance to the question of transition state imbalance. (1) The progress in the C-Y bond contraction. (2) The progress in the planarization of the α -carbon, i.e., the change in the pyramidal angle. (3) The charges on the Y and the CH₂ groups at the transition stage relative to those in CH₃Y and CH₂=Y⁻. The relationship between these charges is conveniently described by the imbalance parameter n defined in eq 12;¹³ δ_Y and δ_C are the transition state charges on Y and CH₂, respectively, while χ is the charge on Y in the anion (eq 13).⁴¹ Equation 12

$$n = \frac{\log(\delta_Y/\chi)}{\log(\delta_C + \delta_Y)} \quad (12)$$

is simply the logarithmic version of eq 14 solved for n . For a balanced transition state, $n = 1$; for an imbalanced transition state where charge delocalization lags behind



$$\delta_Y = \chi(\delta_C + \delta_Y)^n \quad (14)$$

proton transfer, $n > 1$, with n becoming larger with increasing degree of imbalance. We shall return to eq 14 below.

The n values and the % progress in the C-Y bond contraction and planarization of the α -carbon are reported Table 6. There is a good correlation between the two geometric parameters, i.e., increases in $\Delta r_{C-Y}^\ddagger/\Delta r_{C-Y}^\circ$ are reflected in increases in $\Delta\alpha^\ddagger/\Delta\alpha^\circ$. For n one expects an inverse correlation with the geometric parameters, i.e., n is expected to decrease with increasing $\Delta r_{C-Y}^\ddagger/\Delta r_{C-Y}^\circ$ or $\Delta\alpha^\ddagger/\Delta\alpha^\circ$. This is found to be the case, especially with respect to n vs $\Delta\alpha^\ddagger/\Delta\alpha^\circ$. For example, for CH₃C≡CH which has the lowest $100 \times \Delta\alpha^\ddagger/\Delta\alpha^\circ$ value (9.9), n is the highest (2.26); for CH₃NO and CH₂CH=S which have the highest $100 \times \Delta\alpha^\ddagger/\Delta\alpha^\circ$ values (44.0 and 41.0, respectively), n is the lowest (1.28 and 1.42, respectively); for the other seven systems the progress in the planarization

(34) This is similar to results reported in ref 35.

(35) Polásek, M.; Tureček, F. *J. Am. Chem. Soc.* **2000**, *122*, 525.

(36) At MP2/6-311+G(d, p)//MP2/6-31G(d, p), ref 13c.

(37) Note that in ref 13c $\Delta\Delta H^\circ$ was defined as $\Delta H^\circ(\text{CH}_4) - \Delta H^\circ(\text{CH}_3\text{Y})$ which led to positive ρ_R° and ρ_F° values.

(38) Taft, R. W. *Prog. Phys. Org. Chem.* **1983**, *14*, 247.

(39) Van Verth, J. E.; Saunders, W. H., Jr. *J. Org. Chem.* **1997**, *62*, 5743.

(40) Bernasconi, C. F.; Kittredge, K. W. *J. Org. Chem.* **1998**, *63*, 1944.

(41) More precisely, δ_Y and δ_C are defined as the difference in charge between that on the transition state and CH₃Y, and χ as the difference in charge between that on the anion and CH₃Y.¹³

Table 6. Transition States: Imbalance Parameter, Progress in C–Y Bond Contraction and in Planarization of α -Carbon

| CH ₃ Y | n^a | $100 \times (\Delta r_{C-Y}^\ddagger / \Delta r_{C-Y}^o)^b$ | $100 \times (\Delta \alpha^\ddagger / \Delta \alpha^o)^c$ | σ_R^d |
|------------------------------------|-------|---|---|------------------|
| CH ₃ C≡N | 1.51 | 53.3 | 21.2 | 0.10 |
| CH ₃ C≡CH | 2.26 | 34.7 | 9.9 | $\approx 0.15^e$ |
| CH ₃ CH=CH ₂ | 1.61 | 56.3 | 22.6 | 0.16 |
| CH ₃ CH=NH(syn) | 1.58 | 57.0 | 25.8 | $\approx 0.17^e$ |
| CH ₃ CH=NH(anti) | 1.55 | 61.7 | 27.6 | $\approx 0.17^e$ |
| CH ₃ CH=O | 1.52 | 65.2 | 34.1 | 0.19 |
| CH ₃ CH=S | 1.42 | 64.2 | 41.0 | $\approx 0.33^e$ |
| CH ₃ NO ₂ | 1.59 | 57.7 | 26.8 | 0.18 |
| CH ₃ NO | 1.28 | 70.0 | 44.0 | 0.26 |

^a Equation 12. ^b % Progress of C–Y bond contraction at TS. ^c % Change of pyramidal angle at TS. ^d Taft's²³ gas-phase resonance substituent constants. ^e Estimated, see text.

is quite similar and ranges from 21.2 to 27.6 while the n values are also quite similar (1.51 to 1.61).

A question that, until now, has remained unresolved is whether there is a correlation between n and the π -acceptor strength of Y. Earlier, more limited data seemed to support the intuitively appealing notion that n should increase with increasing acceptor strength.^{12b,13c} However, there is no requirement for such a correlation. This is because n measures the lag in charge delocalization relative to the charge developed on the Y-group of the *actual* anion and not relative to a hypothetical anion which has all its negative charge delocalized onto the Y-group. A detailed discussion of this point has been presented elsewhere.^{13b} The results in Table 6 show that there is no correlation of n with the π -acceptor strength as measured by σ_R . In fact the two strongest π -acceptors, CH=S and NO, are associated with the smallest imbalances. At this point we are unable to detail what determines the magnitude of the imbalance except to say that it must be the result of optimizing the contributions from bond changes, from resonance, field, and polarizability effects (see below) as well as from electrostatic/hydrogen bonding effects. These latter are believed to be important¹³ because the proton in flight carries a significant positive charge that can stabilize the negative CH₂ groups.

The unusually large n value for the CH₃C≡CH/CH₂=C=CH[−] system (2.26) calls for comment, though. A factor that may play a role here is that the conversion of propyne to its anion requires a large change in the C≡C–H angle from 180° to 126° (Figure S1),¹⁹ reflecting a change in hybridization of the terminal carbon from sp to something approaching sp². At the transition state, this angle is 171° (Figure S1),¹⁹ indicating that rehybridization has made minimal progress. This difficulty in rehybridizing the terminal carbon before the acidic proton is completely lost may be related to the need to significantly change the position of the hydrogen; it may add to the lag in charge delocalization and hence contribute to the enhanced n value. This situation contrasts with that for other systems where the terminal atom of the Y group carries hydrogen(s), i.e., propene and acetimine. Here the respective C=C–H and C=N–H angles (Figure S1)¹⁹ change very little upon conversion of the carbon acid (125° for propene, 109° for CH₃CH=NH(syn) and CH₃CH=NH(anti)) to the transition state (125° for propene, 107° for CH₃CH=NH(syn), 108° for CH₃CH=NH(anti)) and to the anion (125° for propene, 106° for CH₃CH=NH(syn), 107° for CH₃CH=NH(anti)). Accordingly, these

systems have n values that are all very similar and close to the n values of the systems without hydrogens on the terminal atoms of the Y-group (Table 6).

Intrinsic Barriers. As before,¹³ the barriers (ΔH^\ddagger) are defined as the difference in enthalpy between the transition state and the *separated* reactants.⁴² They are summarized in Table 1 at various computational levels. In view of the fact that the MP2//MP2 calculations on the acidities give the best agreement with the experimental values and/or the ones calculated at the CCSD(T)/6-311+G(2df,2p) level, we will take the MP2//MP2 barriers as the most reliable ones in our further discussion.

On the basis of a suggestion by a reviewer, we have also calculated the barriers including BSSE counterpoise corrections.⁴⁴ They are included in Table 1. The corrections are very small (<1 kcal/mol except for CH₄) and nearly constant at the RHF, B3LYP, and BPW91 levels but more substantial at the MP2 level (mostly 3 to 3.5 kcal/mol). As noted before,^{13c} the fact that at a given level, the corrections depend very little on the particular reaction means that whether they are included or not does not change any of the conclusions of this paper. In view of this and due to the controversy as to whether at the MP2 level the counterpoise method may lead to an overcorrection⁴⁵ our discussion will be mainly based on the uncorrected values.

The barriers for all CH₃Y/CH₂=Y[−] systems are lower than for the CH₄/CH₃[−] system. This means that the stabilization of the transition state by the Y-group is greater than that of the respective anion. The situation is illustrated in Figure 2 (left panel) for the case of CH₃NO₂; it shows that the transition state for the CH₃NO₂ reaction is more stable than the transition state for the methane reaction by 73.3 kcal/mol while CH₂=NO₂[−] is more stable than CH₃[−] by only 59.1 kcal/mol.⁴⁶

The greater stabilization of the transition state compared to the anion may be attributed to the fact that, because the proton in flight is positively charged, each CH₂Y-fragment carries more than half a negative charge (Table 3). This leads to a stronger substituent effect on the transition state than on the anion resulting from the interaction of the Y-group with the negative charges. It also provides additional stabilization by electrostatic/hydrogen bonding effects between the proton in flight and the negative CH₂Y-fragments (more on this in ref 13).

Further insights are obtained by analyzing the relative contributions of field, resonance, and polarizability effects to the barriers. A plot corresponding to eq 15 for the systems with known σ_F , σ_R , and σ_α values, respectively,

(42) In gas-phase ion–molecule reactions the transition state is typically preceded by an ion–dipole complex^{5a,5c,43} formed between the reactants and the term “barrier” is sometimes used for the enthalpy difference between the transition state and this ion–dipole complex. These ion–dipole complexes have little relevance to the main focus of this paper (see, e.g., ref 12b), and we have not included them in our calculations.

(43) Pellerite, M. J.; Brauman, J. I. *J. Am. Chem. Soc.* **1980**, *102*, 5993.

(44) Boys, S. F.; Bernardi, F. *Mol. Phys.* **1970**, *19*, 553.

(45) (a) Cook, D. B.; Sordo, J. A.; Sordo, T. L. *Int. J. Quantum Chem.* **1993**, *48*, 375. (b) Davidson, E. R.; Chakravorty, S. *J. Chem. Phys. Lett.* **1994**, *217*, 48.

(46) Figure 2 is based on the assumption that the entire difference in acidity between CH₃NO₂ and CH₄ (59.1 kcal/mol) is the result of the stabilization of the anion by the nitro group. This is probably a good approximation. Note, however, that the calculated 14.2 (73.3–59.1) kcal/mol additional stabilization of the transition state compared to the stabilization of the nitronate anion does not depend on this approximation.

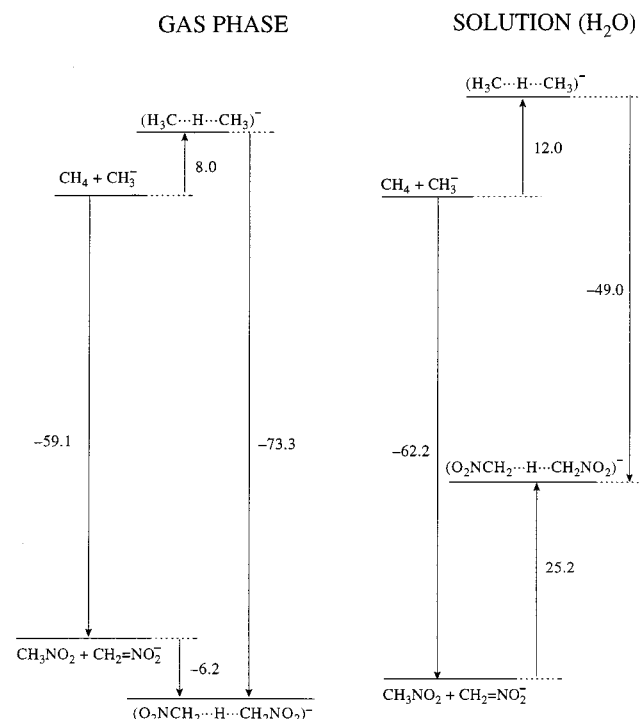


Figure 2. Stabilization of $\text{CH}_2=\text{NO}_2^-$ relative to CH_3^- and of the transition state of the $\text{CH}_3\text{NO}_2/\text{CH}_2=\text{NO}_2^-$ reaction relative to the transition state of the $\text{CH}_4/\text{CH}_3^-$ reaction in the gas phase and in aqueous solution.

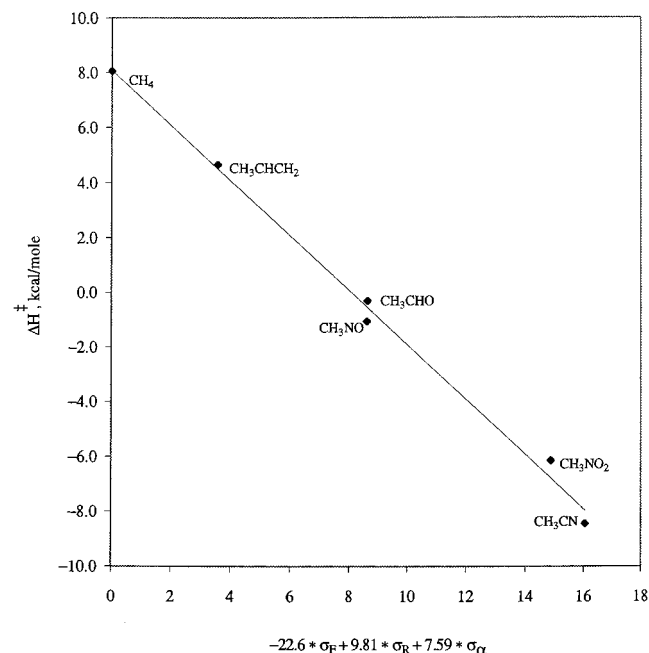


Figure 3. Plot of ΔH^\ddagger vs $\rho_F^\ddagger\sigma_F + \rho_R^\ddagger\sigma_R + \rho_\alpha^\ddagger\sigma_\alpha$; ρ -values obtained by least-squares fitting ($r^2 = 0.995$, intercept = 8.08).

$$\Delta\Delta H^\ddagger = \Delta H^\ddagger(\text{CH}_3\text{Y}) - \Delta H^\ddagger(\text{CH}_4) = \rho_F^\ddagger\sigma_F + \rho_R^\ddagger\sigma_R + \rho_\alpha^\ddagger\sigma_\alpha \quad (15)$$

is shown in Figure 3. The correlation is excellent ($r^2 = 0.995$) and yields $\rho_F^\ddagger = -22.6$, $\rho_R^\ddagger = 9.81$, and $\rho_\alpha^\ddagger = 7.59$. These ρ -values indicate that the field and polarizability effects⁴⁷ are barrier reducing, the resonance effect barrier enhancing. A previous correlation without the $\rho_\alpha^\ddagger\sigma_\alpha$ term and without data for CH_3NO yielded $\rho_F^\ddagger = -25.8$ and

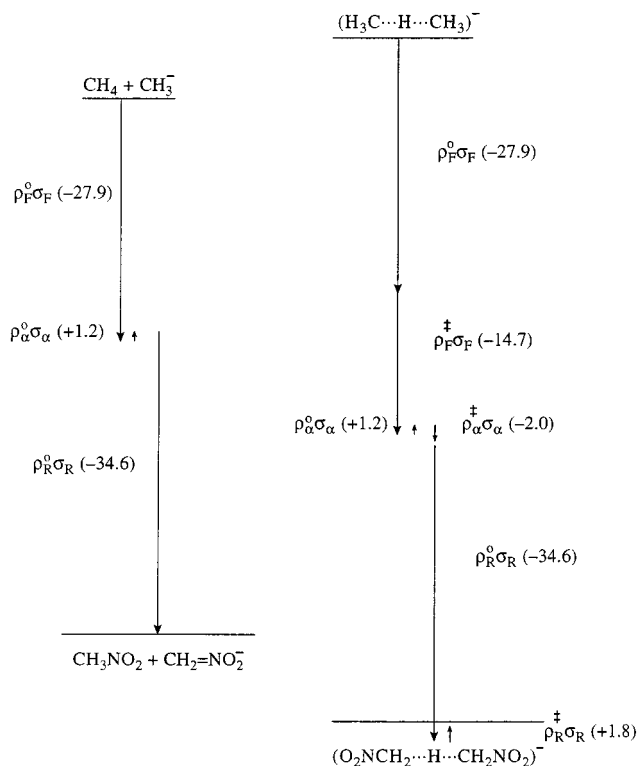


Figure 4. Contributions of the field, resonance, and polarizability effects to the stabilization (destabilization) of $\text{CH}_2=\text{N O}_2^-$ relative to CH_3^- and of the transition state of the $\text{CH}_3\text{NO}_2/\text{CH}_2=\text{NO}_2^-$ reaction relative to the transition state of the $\text{CH}_4/\text{CH}_3^-$ reaction in the gas phase.

$\rho_R^\ddagger = -6.7$ ($r^2 = 0.995$).^{13c} For the BSSE-corrected MP2 barriers the correlation (Figure S3¹⁹) yields $\rho_F^\ddagger = -23.6$, $\rho_F^\ddagger = 7.38$ and $\rho_\alpha^\ddagger = 7.82$ ($r^2 = 0.993$). For the B3LYP barrier (Figure S4¹⁹) one obtains $\rho_F^\ddagger = -22.9$, $\rho_F^\ddagger = -3.85$ and $\rho_\alpha^\ddagger = 0.78$ but the correlation ($r^2 = 0.985$) is not as good as for the MP2 barriers; for the BSSE corrected B3LYP barriers the correlation (Figure S5¹⁹) yields $\rho_F^\ddagger = -24.7$, $\rho_F^\ddagger = -5.32$ and $\rho_\alpha^\ddagger = 0.47$ ($r^2 = 0.984$).

In Table 5 the individual $\rho_F^\ddagger\sigma_F$, $\rho_R^\ddagger\sigma_R$, and $\rho_\alpha^\ddagger\sigma_\alpha$ terms are reported for each system, allowing a detailed assessment of the relative contribution of the resonance, field, and polarizability effects to the reduction of the intrinsic barriers relative to that of the $\text{CH}_4/\text{CH}_3^-$ system. The following points are noteworthy.

(1) For all systems except $\text{CH}_3\text{CH}=\text{CH}_2$ and $\text{CH}_3\text{CH}=\text{S}$, the field effect is dominant and lowers the barrier by substantial amounts (-7.0 to -14.7 kcal/mol). The barrier lowering effect results from the fact that the transition state stabilization corresponds to $\rho_F^\ddagger\sigma_F + \rho_F^\ddagger\sigma_F$, i.e., the field effect on the transition state is $(\rho_F^\ddagger + \rho_F^\ddagger)/\rho_F^\ddagger = (-43.0 - 22.6)/(-43.0) = 1.52$ -fold stronger than on the anion. This is illustrated in Figure 4 for the case of CH_3NO_2 .

(2) The polarizability effect contributes -1.9 to -5.7 kcal/mol to the lowering of the barrier. For most cases this is a minor contribution compared to that of the field effect; for $\text{CH}_3\text{C}\equiv\text{CH}$ and $\text{CH}_3\text{CH}=\text{S}$ it is comparable to the field effect while for $\text{CH}_3\text{CH}=\text{CH}_2$ it is the dominant factor. The lowering of the barrier by the polarizability

(47) Since the σ_α values are negative,²³ a positive ρ_α^\ddagger means $\rho_\alpha^\ddagger\sigma_\alpha < 0$ (barrier lowering).

effect comes about because the stabilization of the transition state, which is given by $\rho_{\alpha}^{\circ}\sigma_{\alpha} + \rho_{\alpha}^{\ddagger}\sigma_{\alpha}$ (Figure 4), more than offsets the destabilization of the anion ($\rho_{\alpha}^{\circ} = -4.6$, $\rho_{\alpha}^{\ddagger} = 7.59$). The fact that the transition states, which have less charge on the Y group than the anions, are stabilized but that the anions are destabilized (or hardly affected) supports our conclusion that the polarizability effect is greatly reduced when the Y group carries a large negative charge. Since even for the transition states there is significant negative charge on the Y group, the polarizability effect on their stability is rather modest. This contrasts with the reactions of the type $\text{ZCH}_3 + \text{ZCH}_2^- \rightleftharpoons \text{ZCH}_2 + \text{ZCH}_3$ with $\text{Z} = \text{F}, \text{Cl}, \text{Br}, \text{OH}, \text{SH}$ where the polarizability of Z has a strong barrier reducing effect.³⁹

(3) The resonance effect increases the barriers by 1.0 to 3.2 kcal/mol. The reason for this small increase is that the resonance stabilization of the transition state which is given by $\rho_{\text{R}}^{\circ}\sigma_{\text{R}} + \rho_{\text{R}}^{\ddagger}\sigma_{\text{R}}$ (Figure 4) is only $(\rho_{\text{R}}^{\circ} + \rho_{\text{R}}^{\ddagger})/\rho_{\text{R}}^{\circ} = (-192.5 + 9.81)/(-192.5) = 0.95$ as strong as that of the anion.

The finding that the resonance effect slightly increases the barriers should not be viewed as a significant contradiction of our earlier report according to which the resonance effect slightly *lowers* the barriers.^{13c} This is because the focus has to be on how resonance affects *transition state stability*, and here there is no major difference between the present conclusion that 95% of the anion stabilization is reflected in the transition state compared to the earlier figure of 104%.^{13c} Because both figures are close to 100%, a difference of just a few percent will either translate into a slight barrier enhancing or reducing effect. The observed difference between the present and previous results is mainly a consequence of including polarizability effects into our correlations.

A finding that *is* significant is that there is substantial transition state stabilization by resonance but the degree of resonance stabilization of the transition state relative to the anion (95%) is significantly less than the degree of stabilization of the transition state by the field effect relative to the anion (152%). The lower figure for the resonance effect is, of course, a consequence of the imbalance which prevents the resonance effect from being as strongly developed as the field effect.

Estimate of Substituent Constants for $\text{C}\equiv\text{CH}$, $\text{CH}=\text{NH}$, and $\text{CH}=\text{S}$. No gas-phase substituent constants have been reported for $\text{CH}=\text{NH}$ and $\text{CH}=\text{S}$; for $\text{C}\equiv\text{CH}$ Taft and Topsom^{23a} report $\sigma_{\text{F}} = 0.23$, $\sigma_{\text{R}} = 0.00$, and $\sigma_{\alpha} = -0.60$, a set which does not seem "reasonable," mainly because it implies that $\text{C}\equiv\text{CH}$ has no π -acceptor ability. Our study allows us to estimate σ_{F} , σ_{R} , and σ_{α} for $\text{C}\equiv\text{CH}$, $\text{CH}=\text{NH}$, and $\text{CH}=\text{S}$ as follows.

A plot of σ_{R} vs $\Delta I_{\text{C}-\text{Y}}^{\circ}/I_{\text{C}-\text{Y}}$ (not shown) for CN, $\text{CH}=\text{CH}_2$, $\text{CH}=\text{O}$, and NO gives a good linear correlation with a slope $= 2.41 \pm 0.12$ ($r^2 = 0.996$) and negligible intercept.⁴⁸ If one assumes that $\text{C}\equiv\text{CH}$, $\text{CH}=\text{NH}$, and $\text{CH}=\text{S}$ conform to the same plot, one can calculate the σ_{R} values reported in Tables 4–6. If one further assumes that the acidities and barriers for $\text{CH}_3\text{C}\equiv\text{CH}$, $\text{CH}_3\text{CH}=\text{NH}$, and $\text{CH}_3\text{CH}=\text{S}$ follow the correlations of Figures 1 and 3, respectively, a set of σ_{F} and σ_{α} can be found that reproduce the acidities and at the same time correlate reasonably well with the barriers.

These σ_{F} and σ_{α} values are summarized in Table 5 for $\text{C}\equiv\text{CH}$, $\text{CH}=\text{NH}(\text{syn})$ and $\text{CH}=\text{NH}(\text{anti})$, along with $\rho_{\text{F}}^{\circ}\sigma_{\text{F}}$, $\rho_{\text{F}}^{\ddagger}\sigma_{\text{F}}$, $\rho_{\text{R}}^{\circ}\sigma_{\text{R}}$, $\rho_{\text{R}}^{\ddagger}\sigma_{\text{R}}$, $\rho_{\alpha}^{\circ}\sigma_{\alpha}$, and $\rho_{\alpha}^{\ddagger}\sigma_{\alpha}$. For $\text{CH}=\text{S}$ no set of "reasonable" σ_{F} and σ_{α} values could be found that would, together with σ_{R} (0.22) calculated by the above method, give a good correlation. However, a good correlation is found if one assumes a larger σ_{R} (0.33); the resulting σ_{F} and σ_{α} for $\text{CH}=\text{S}$ values seem "reasonable," i.e., σ_{F} is smaller than for $\text{CH}=\text{O}$, reflecting the lower electronegativity of sulfur, and σ_{α} is larger than for $\text{CH}=\text{O}$, reflecting the stronger polarizability of sulfur. The estimated substituent constants for $\text{C}\equiv\text{CH}$ and $\text{CH}=\text{NH}(\text{syn})$ also appear to fit with qualitative expectations. Specifically, σ_{F} for $\text{C}\equiv\text{CH}$ (0.14) is higher than for $\text{CH}=\text{CH}_2$ (0.06), reflecting the fact that sp carbon is more electronegative than sp² carbon; σ_{F} for $\text{CH}=\text{NH}(\text{syn})$ (0.27) is lower than for $\text{CH}=\text{O}$ (0.31) but higher than for $\text{CH}=\text{S}$ (0.22), again reflecting electronegativities; σ_{α} for $\text{C}\equiv\text{CH}$ (−0.40) is somewhat lower than for $\text{CH}=\text{CH}_2$ (−0.50), consistent with the greater hardness of sp compared to sp² carbon. The significantly lower σ_{F} (0.20) for $\text{CH}=\text{NH}(\text{anti})$ compared to $\text{CH}=\text{NH}(\text{syn})$ (0.27) is surprising, though, and we have no explanation for it except to say that for *all* the estimated substituent constants their approximate nature needs to be kept in mind.

The one Y group for which no set of σ_{F} , σ_{R} , and σ_{α} values is able to satisfactorily reproduce *both* ΔH° and ΔH^{\ddagger} is $\text{C}\equiv\text{CH}$. The σ_{F} , σ_{R} , and σ_{α} values that give an acidity within 0.5 kcal/mol of its MP2 value lead to a barrier that is 1.6 kcal/mol higher than the MP2 value. This discrepancy is significantly larger than for all the other Y groups. It may be related to the unusually large imbalance for the $\text{CH}_3\text{C}\equiv\text{CH}/\text{CH}_2=\text{C}=\text{CH}^-$ system. This large imbalance results from a disproportionately large negative charge on the CH_2 group at the transition state (Table 3). This should render the transition state more responsive to the stabilization by the field and polarizability effects, and less responsive to the destabilization by the resonance effect of the $\text{C}\equiv\text{CH}$ group. The result is a barrier that is lower than that based on the $\rho_{\text{F}}^{\ddagger}$, $\rho_{\text{R}}^{\ddagger}$, and ρ_{α}^{\ddagger} .

Solution versus Gas-Phase Proton Transfer. Our analysis shows that the field and/or resonance effects are the dominant factors in stabilizing the anions and transition states in the gas phase. In solution, these factors are important, too, but solvation, especially of the anion, is often a dominant force. This leads to significant differences in how barriers are affected by Y in the gas phase and in solution. In the gas phase the Y-group lowers the barrier because it stabilizes the transition state more than the anion. This can be traced to the field effect which is 52% more effective in stabilizing the transition state than the anion. Since the resonance effect on the transition state is almost as strong as on the anion (95%) and hence leads only to a marginal barrier increase, the net result is a barrier reduction.

For solution proton transfers the situation is reversed, i.e., the Y-group increases the barrier because it stabilizes the transition state *less* than the anion. This is illustrated in Figure 2 (right panel) for the example of the $\text{CH}_3\text{NO}_2/\text{CH}_2=\text{NO}_2^-$ system where the reactants are stabilized by ~ 62.2 kcal/mol relative to $\text{CH}_4/\text{CH}_3^-$ ⁴⁹ while the transi-

(48) NO_2 deviates from this correlation and has not been included in determining the slope.

(49) Based on $\text{pK}_{\text{a}}^{\text{CH}_4} \approx 56^{50}$ and $\text{pK}_{\text{a}}^{\text{CH}_3\text{NO}_2} = 10.3^{51}$. Note that remarks similar to those in ref 46 apply here.

tion state for the $\text{CH}_3\text{NO}_2/\text{CH}_2=\text{NO}_2^-$ reaction is stabilized by ~ 49.0 kcal/mol relative to the transition state of the $\text{CH}_4/\text{CH}_3^-$ reaction.⁵² Note that the energies in Figure 2 for the solution reaction refer to Gibbs free energies rather than enthalpies; the latter are not available.

The stronger solvation of the anion compared to that of the transition state, especially the hydrogen bond solvation of the nitro group, is likely to be the main reason for this reversal. Furthermore, if the degree of transition state stabilization by the field and resonance effects represents a smaller percentage of the anion stabilization than is the case in the gas phase, this would contribute to the reversal. This is probably the case although a quantitative assessment of this notion is difficult to come by. Nevertheless, when solvation and resonance are treated together, a back of the envelope type calculation suggests that their combined effect on the transition state may be less than 40% of their combined effect on the anion.^{9c}

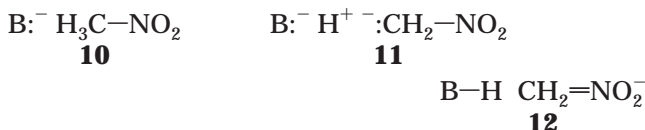
Why Are the Transition States Imbalanced? This question continues to generate interest and controversy,^{14,54} hence some comments and clarifications are in order. The explanation that we have favored is based on a simple and intuitively appealing model initially proposed by Kresge⁵⁵ in the context of proton transfers from nitroalkanes, a model that we have applied to the generalized reaction scheme of eq 13. The basic idea is that delocalization of negative charge into the Y group can only occur if there is development of the C–Y π -bond. Hence the fraction of charge on Y depends on the fraction of π -bond formation and α -carbon rehybridization, and the fraction of π -bond formation in turn depends on the fraction of charge transferred from the base to the carbon acid. This means that the charge on Y cannot be very large since it represents only a fraction of a fraction. This model is the basis of eq 12 which defines the degree of imbalance, n .^{9c,13a}

In a recent paper, Saunders et al.^{54b} state that “it has never been clear why the reaction should choose this energy path⁵⁶ when the fully synchronous and presumably lower-energy path seemed in principle to be avail-

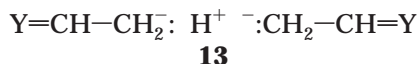
able. If more delocalization and hence more stabilization could be gained by more complete rehybridization in the transition state, why is rehybridization as limited as it is?”

We believe the answers to these questions are an implicit part of the Kresge model. The point is that the fully synchronous path is *not* available and not of lower but of higher energy. This is because whatever extra transition state stabilization might come from more complete delocalization is more than offset by the *increase* in energy resulting from forcing more negative charge into Y without the underpinnings of a more completely formed C–Y π -bond and/or from forcing the formation of a more complete π -bond without providing enough charge from the base to do so. The calculation of a hypothetical, more-delocalized transition state for the reaction of $\text{CH}_2\text{CH}=\text{O}/\text{CH}_2=\text{CHO}^-$ puts this argument on a more quantitative footing:^{13a} constraining the α -carbon to a planar geometry indeed results in a more complete π -bond formation and more extensive charge delocalization, but the energy is 10.5 kcal/mol higher than for the actual, fully optimized, transition state.^{13a} A similarly constrained transition state for the $\text{CH}_3\text{NO}_2/\text{CH}_2=\text{NO}_2^-$ system was found to be 16.9 kcal/mol higher in energy than the actual transition state.^{13c} Thus the actual transition state will always be the one whose energy is minimized by the best mix of resonance, field, and polarizability effects as well as electrostatic/hydrogen bonding effects.

A different approach which leads to the same answer was proposed by Pross and Shaik.⁵⁷ They view the transition state as a hybrid of the three resonance structures **10**, **11**, and **12**, with the triple ion species **11** making an important contribution to the hybrid. Without **11**, the transition state would be akin to the above-



mentioned hypothetical transition state calculated by constraining it to be more delocalized. The mixing in of **11** into the resonance hybrid both stabilizes the transition state and explains the localization of the negative charge on the carbon. Clearly, both the Kresge and the Pross/Shaik model lead to identical conclusions. Recent calculations utilizing valence bond self-consistent field (VBSCF) methods⁵⁴ have confirmed the importance of triple ion structures such as **13** as contributors to the resonance hybrid of the transition state in the $\text{CH}_3\text{CH}=\text{O}/\text{CH}_2=\text{CHO}^-$ and $\text{CH}_3\text{CH}=\text{CH}_2/\text{CH}_2=\text{CH}_2^-$ systems.



Conclusions

(1) The acidities of CH_3Y are mainly determined by the resonance and/or field effects of Y. The polarizability of Y plays an insignificant role, probably because a large fraction of the anionic charge is on the Y group.

(2) The π -acceptor strength of the $\text{C}\equiv\text{CH}$ group is significantly greater than that of the CN group, despite

(50) Bordwell, F. G. *Acc. Chem. Res.* **1988**, *21*, 457.

(51) Bernasconi, C. F.; Klinier, D. A. V.; Mullin, A. S.; Ni, J. X. *J. Org. Chem.* **1988**, *53*, 3342.

(52) $\Delta G^\ddagger \approx 12$ kcal/mol for the intrinsic barrier of the reaction $\text{CH}_4 + \text{CH}_3^-$ is based on the assumption that the reaction in water has a similar intrinsic barrier as in the gas phase. The value of 12 kcal/mol is 4.5 kcal/mol higher than ΔH^\ddagger because it includes an entropy term. $\Delta G^\ddagger \approx 25.2$ kcal/mol for the reaction $\text{CH}_3\text{NO}_2 + \text{CH}_2=\text{NO}_2^-$ in water was estimated as follows. For the reaction of $\text{PhCH}_2\text{NO}_2 + \text{PhCH}=\text{NO}_2^-$ in 90% DMSO–10% water $\Delta G^\ddagger \approx 20.2$ kcal/mol,^{53a} for the reaction of $\text{CH}_3\text{NO}_2 + \text{PhCH}=\text{NO}_2^-$ in the same solvent, $\Delta G^\ddagger \approx 18.4$ kcal/mol.^{53b} Applying the Marcus equation¹¹ that relates intrinsic barriers of cross reactions to the intrinsic barriers of identity reactions one obtains $\Delta G^\ddagger = 16.6$ kcal/mol for the reaction of $\text{CH}_3\text{NO}_2 + \text{CH}_2=\text{NO}_2^-$. For the reaction of CH_3NO_2 with secondary alicyclic amines, the increased solvation of $\text{CH}_2=\text{NO}_2^-$ in water compared to 90% DMSO–10% water was estimated to contribute 4.3 kcal/mol to the increase in ΔG^\ddagger .^{9c} This suggests that the contribution to the increase in ΔG^\ddagger in a reaction where there is both delayed solvation of the incipient product $\text{CH}_2=\text{NO}_2^-$ as well as early desolvation of the reactant $\text{CH}_2=\text{NO}_2^-$ should be twice as large, i.e., ≈ 8.6 kcal/mol. Thus ΔG^\ddagger for the reaction $\text{CH}_3\text{NO}_2 + \text{CH}_2=\text{NO}_2^-$ in water is estimated at 25.2 kcal/mol.

(53) (a) Bernasconi, C. F.; Ni, J. X. *J. Am. Chem. Soc.* **1993**, *115*, 5060. (b) Bernasconi, C. F.; Ni, J. X. *J. Org. Chem.* **1994**, *59*, 4910.

(54) (a) Harris, N.; Wei, W.; Saunders, W. H., Jr.; Shaik, S. *J. Phys. Org. Chem.* **1999**, *12*, 259. (b) Harris, N.; Wei, W.; Saunders, W. H., Jr.; Shaik, S. *J. Am. Chem. Soc.* **2000**, *112*, 6754.

(55) Kresge, A. J. *Can. J. Chem.* **1974**, *52*, 1897.

(56) The nonsynchronous energy path with the imbalanced transition state.

(57) Pross, A.; Shaik, S. S. *J. Am. Chem. Soc.* **1982**, *104*, 1129.

the greater electronegativity of nitrogen than carbon which presumably should favor delocalization of the negative charge onto the nitrogen of CH_2CN^- . A similar situation is observed for $\text{CH}=\text{O}$ vs $\text{CH}=\text{S}$, the latter being a stronger π -acceptor than the former despite the lower electronegativity of sulfur. The main reason for these "unexpected" findings is that the conversion of a $\text{C}\equiv\text{X}$ triple bond to a $\text{C}=\text{X}$ double bond, or a $\text{C}=\text{X}$ double bond to a $\text{C}-\text{X}$ single bond becomes increasingly less favorable as the electronegativity of X increases, reflecting the greater increase in $\text{C}\equiv\text{X}$ triple bond ($\text{C}=\text{X}$ double bond) strength relative to the $\text{C}=\text{X}$ double bond ($\text{C}-\text{Y}$ single bond) with increasing electronegativity of X. In the case of $\text{CH}_3\text{CH}=\text{S}$, the larger size of the sulfur atom probably contributes to the stabilization of the anion.

(3) The reactions of eq 1 all have imbalanced transition states. However, contrary to earlier suggestions, there is no correlation between the degree of imbalance, measured by n , $\Delta r_{\text{C}-\text{Y}}^\ddagger/\Delta r_{\text{C}-\text{Y}}^\circ$ or $\Delta\alpha^\ddagger/\Delta\alpha^\circ$, and π -acceptor strength of the Y group. As discussed in a previous paper, there is nothing which would *require* such a correlation.

(4) The barriers are all lower than for the $\text{CH}_4/\text{CH}_3^-$ system, indicating that the stabilization of the transition state by the Y-group is greater than that of the respective anion. This enhanced transition state stabilization is mainly the result of an exalted field effect of Y on the large negative charge of the CH_2Y fragments caused by the highly positive proton in flight. For the $\text{CH}_3\text{CH}=\text{CH}_2^-/\text{CH}_2=\text{CHCH}_2^-$ system, the field effect is not very important; here the polarizability effect on the transition state is the dominant factor responsible for lowering the barrier below that of the $\text{CH}_4/\text{CH}_3^-$ system. For the other systems, the polarizability effect plays a minor role.

(5) The resonance effect leads to a small increase in the barrier because, due to the imbalance, the transition state is not quite as strongly stabilized as the anion. However, the small increase is more than offset by the barrier reducing field effect and, to a lesser extent, by the polarizability effect.

(6) For the reactions of eq 1 conducted in aqueous solution, the situation is reversed in the sense that the

Y group *increases* the barrier because it stabilizes the transition state *less* than the anion. This is mainly the result of the stronger solvation of the anion than that of the transition state.

(7) The reasons why the transition states are imbalanced can be equally well understood in the framework of either the Kresge model or the Shaik/Pross model. In both models the localization of the negative charge on the carbon provides a lower energy path than a more complete charge delocalization into the Y group. In the Kresge model the extra stabilization that might come from a more complete delocalization is more than offset by the increase in energy resulting from forcing the transition state into a structure that would require a more complete charge transfer from the base to be sustainable. In the Pross/Shaik model the transition state is viewed as a resonance hybrid whose energy can be lowered by mixing in the triple ion resonance structure (11).

(8) Our study also allowed us to estimate σ_{F} , σ_{R} , and σ_{α} for the Y groups for which no such parameters have been reported yet ($\text{CH}=\text{NH}$, $\text{CH}=\text{S}$, and $\text{C}\equiv\text{CH}$).

Acknowledgment. Acknowledgment is made to the donors of the Petroleum Research Fund, administered by the ACS, for support of this research (Grant PRF 33143-AC4). The frequency analysis of the transition states were run on CUBANE at the University of California, Los Angeles Chemistry Department. We thank Professor Kendall N. Houk for his permission to use this platform. We thank Mike D. Bartberger for his help and suggestions.

Supporting Information Available: Tables S1 (energies), S2 (charges), and S3 (DFT results on bond contractions and charges on Y), and Figures S1 (geometries), S2 (B3LYP correlation of ΔH° with σ_{F} , σ_{R} , and σ_{α}), S3 (MP2 correlation of BSSE-corrected ΔH^\ddagger with σ_{F} , σ_{R} , and σ_{α}), S4 (B3LYP correlation of ΔH^\ddagger with σ_{F} , σ_{R} , and σ_{α}), and S5 (B3LYP correlation of BSSE-corrected ΔH^\ddagger with σ_{F} , σ_{R} , and σ_{α}). This material is available free of charge via the Internet at <http://pubs.acs.org>.

JO001543U